

# SEISMIC RESPONSE CONTROL OF BUILDING STRUCTURE BY FUZZY OPTIMAL LOGIC (SHAKING TABLE TESTS AND SIMULATIONS)

HIDEO FUJITANI<sup>1)</sup>, TOSHIYASU MIYOSHI<sup>2)</sup>, HIROSHI KAWAMURA<sup>3)</sup>  
AKINORI TANI<sup>3)</sup> and TAKASHI MOCHIO<sup>4)</sup>

- 1)Structural Engineering Department, Building Research Institute, Ministry of Construction,  
1 Tatehara, Tsukuba, Ibaraki, JAPAN 305
- 2)Civil Engineering Divisions Group, Penta-Ocean Construction Co.,Ltd.  
3-7-1 Nishi-Shinjuku, Shinjuku-ku, Tokyo, JAPAN 163-10
- 3)Department of Architecture and Civil Engineering, Faculty of Engineering, Kobe University,  
Rokkodai, Nada-ku, Kobe, Hyogo, JAPAN 657
- 4)Nagasaki Research & Development Center, Mitsubishi Heavy Industries, LTD,  
5-717-1, Fukahori, Nagasaki, JAPAN 851-03



Copyright © 1996 Elsevier Science Ltd  
*Paper No. 1805. (quote when citing this article)*  
Eleventh World Conference on Earthquake Engineering  
ISBN: 0 08 042822 3

## ABSTRACT

This Paper outlines shaking table tests and their results for an active seismic response control system that uses fuzzy optimal logic(FOL). The shaking table test results confirmed the validity of the vibration control effect of this seismic response control system. The results of this study lead to two conclusions, that the effectiveness of this FOL control system can be increased by modifying the membership function, and that the results of seismic response control tests can be qualitatively evaluated by two simulation methods.

## KEYWORDS

Shaking table test; Seismic control; Fuzzy optimal logic; Membership function; Maximizing decision

## INTRODUCTION

In building structures, it is generally difficult to construct control systems due to the vast number of unknown variables (such as the type of structure, material, and construction), as well as the deterioration of the structural performance with time. To control the vibration of a structure subjected to earthquakes, a fast response time is critical and must include the time from sensing external excitation to putting actuators in operation. Furthermore there are uncertainties in the input signals to a control system caused by many factors, such as the direction of input ground motion and the location of sensors.

On the premise of these conditions, a series of studies were conducted to evaluate the effectiveness of a seismic response control system that uses fuzzy optimal logic (FOL)<sup>[1]</sup>. To verify the validity and applicability of such a control system, a series of shaking table tests were done on a physical model of a building structure, and the response of the physical model was simulated numerically. This paper outlines these tests and compares the experimental results with the simulated results.

## FOL SEISMIC RESPONSE CONTROL SYSTEM

## Outline of Control System

Figure 1 shows a flow diagram of the FOL seismic response control system used in this study which predicts the input earthquake motion, identifies the structural characteristics of the building in real time, and then optimizes the control variables<sup>[1]</sup>. The algorithm used in this system incorporates fuzzy logic into the earthquake motion prediction<sup>[2]</sup> and control variable optimization, so that uncertain or fuzzy phenomena can be handled rationally<sup>[3]</sup>. This FOL system uses an active seismic response control method that combines the equivalent loading-term variable mass method, where the controlling force acts for the inertia force, and the equivalent variable viscosity method, where the controlling force acts for viscous damping. The former method reduces the influence of input earthquake motion, and the latter increases the damping by viscosity.

## Equations of Motion

The following equations of motion were used for 2-degrees-of-freedom FOL control system.

$$m_2 \ddot{y}_2 + c_2 (\dot{y}_2 - \dot{y}_1) + k_2 (y_2 - y_1) + u_d - u_m = -m_2 \ddot{z}_0 \quad \dots(1)$$

$$m_1 \ddot{y}_1 + c_1 \dot{y}_1 - c_2 (\dot{y}_2 - \dot{y}_1) + k_1 y_1 - k_2 (y_2 - y_1) = -m_1 \ddot{z}_0 \quad \dots(2)$$

$$u_d = \Delta c \dot{y}_2 \quad \dots(3), \quad u_m = \alpha m_2 \ddot{z}_0 \quad \dots(4)$$

where  $m$  is the mass,  $c$  is the viscous damping coefficient,  $k$  is the spring coefficient,  $y$  is the relative displacement,  $\ddot{z}_0$  is the acceleration of earthquake ground motion,  $u_d$  is the controlling force acting for viscous damping,  $\Delta c$  is the coefficient of additional viscous damping,  $u_m$  is the controlling force acting for external inertia force, and  $\alpha$  is the reduction factor, and the subjects, 0, 1, and 2, denote ground floor, second floor, and uppermost floor respectively.

## Control Algorithm

### (1) Identification of the Structure

In this FOL control system, the maximum response displacement  $Y$  of the uppermost floor is the maximum absolute value  $y$  during the control period  $\Delta t_i$  (shown in Figure 2) and is determined by a trade-off between the controlling forces  $U_{m_i}$  and  $U_{d_i}$  which are the maximum absolute values of  $u_{m_i}$  and  $u_{d_i}$  during  $\Delta t_i$ . In the identification of the structure, the following equations are used:

$$Y_{i-1} = a_{i-1} (1 - \alpha_{i-1}) X_{i-1} / \Delta c_{i-1} \quad \dots(5), \quad Y_i = a_i (1 - \alpha_i) X_i / \Delta c_i \quad \dots(6)$$

$$\dot{Y}_{i-1} = b_{i-1} (1 - \alpha_{i-1}) X_{i-1} / \Delta c_{i-1} \quad \dots(7), \quad \dot{Y}_i = b_i (1 - \alpha_i) X_i / \Delta c_i \quad \dots(8)$$

where,  $X_{i-1}$  and  $X_i$  is the predicted maximum absolute value of input earthquake motion,  $a_{i-1}, a_i, b_{i-1}$  and  $b_i$  are calculated from the response, for the  $(i-1)$ -th and  $i$ -th control periods. From the values thus obtained, predicted values of the maximum response displacement  $Y_{i+1}$  and the maximum response velocity  $\dot{Y}_{i+1}$  for the  $(i+1)$ -th control period are calculated using the following equations:

$$a_{i+1} = (a_{i-1} + a_i) / 2 \quad \dots(9), \quad b_{i+1} = (b_{i-1} + b_i) / 2 \quad \dots(10)$$

$$Y_{i+1} = a_{i+1} (1 - \alpha_{i+1}) X_{i+1} / \Delta c_{i+1} \quad \dots(11), \quad \dot{Y}_{i+1} = b_{i+1} (1 - \alpha_{i+1}) X_{i+1} / \Delta c_{i+1} \quad \dots(12)$$

The predicted maximum values of the controlling forces,  $U_{m_{i+1}}$  and  $U_{d_{i+1}}$  in the  $(i+1)$ -th control period are calculated as follows:

$$U_{m_{i+1}} = \alpha_{i+1} m_2 X_{i+1} \quad \dots(13), \quad U_{d_{i+1}} = \Delta c_{i+1} \dot{Y}_{i+1} = b_{i+1} (1 - \alpha_{i+1}) X_{i+1} \quad \dots(14)$$

### (2) Control Value Optimization by Maximizing Decision

The maximizing decision is where the algorithm determines the optimal values of  $\alpha$  and  $\Delta c$ . In this decision, the membership function (MF) shown in Figure 2 is defined for the maximum response displacement ( $Y$ ) and the maximum controlling force ( $U$ ). With respect to  $U$ , the maximum value  $U'_{i+1}$  in the control period  $\Delta t_{i+1}$  is defined as

$$U'_{i+1} = \sqrt{U_{d_{i+1}}^2 + U_{m_{i+1}}^2} \quad \dots(15)$$

The values of  $\alpha$  and  $\Delta c$  need to be determined simultaneously using Eq. (11) and the MF for  $Y$ , shown in Figure 3(a) and Eq. (11), and the MF for  $U$ , shown in Figure 3(b) and Eq. (15). By using Eqs. (11)-(15),  $Y_{i+1}$  and  $U'_{i+1}$  are transformed into the  $\alpha_{i+1}(\Delta c_{i+1})$  plane (shown in Figure 4). The resulting  $\mu^*$  and  $\alpha^*$  ( $\Delta c^*$ ) are the optimal membership degree and the optimal control variable, respectively.

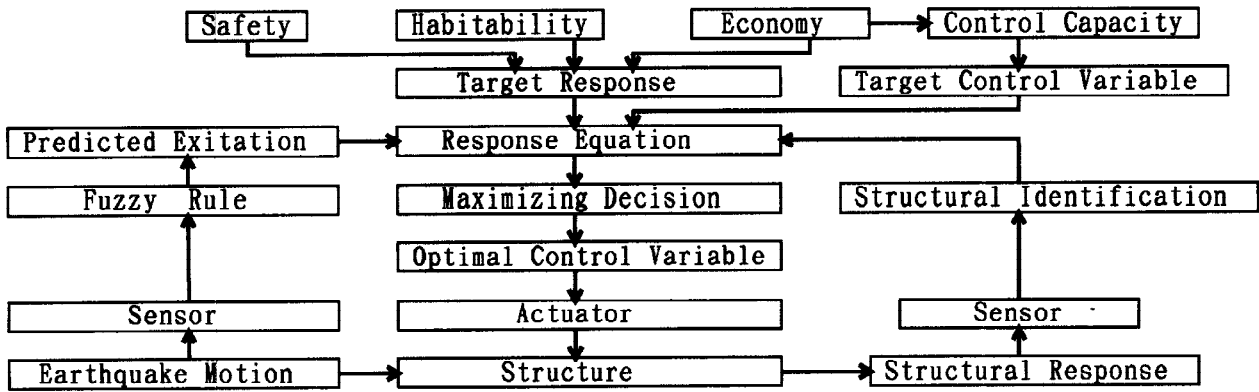


Fig.1 Flow Diagram of the FOL Seismic Response Control System

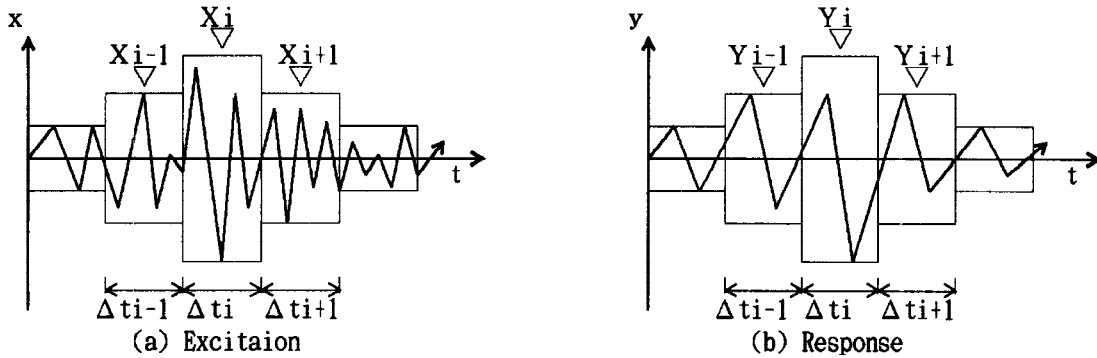


Fig.2 Excitation and Response

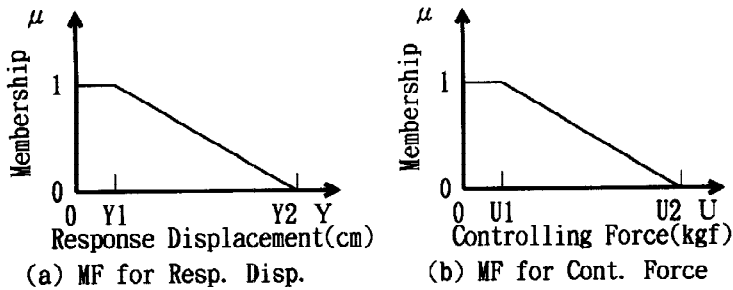


Fig.3 Membership Function

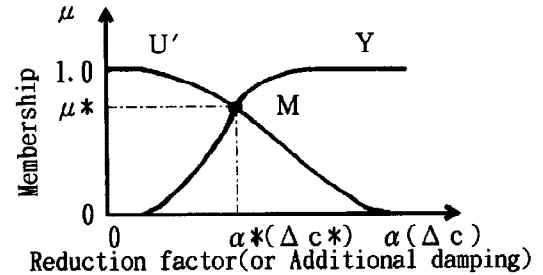


Fig.4 Optimal  $\alpha(\Delta c)$  by Maximizing Decision

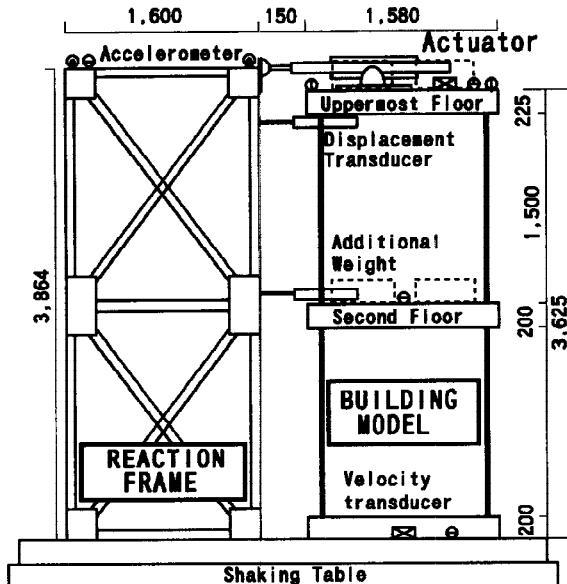


Fig.5 Testing Device and the Positions of Sensors

Table 1 Specification of Model

Component	Specification
Floors	<ul style="list-style-type: none"> <li>Composed of steel plates, H-shaped steels and additional weights</li> <li>Dimension of Plan : about 1580x1080 mm</li> <li>Weight of 2F : 2.027 ton</li> <li>Weight of RF : 2.030 ton</li> </ul>
Columns	<ul style="list-style-type: none"> <li>Four Columns for Each Story</li> <li>Dimension of Cross Section : 19x235mm</li> <li>Height : 1500mm</li> </ul>

Table 2 Control Facilities

Component	Types or Specification
Sensor	<ul style="list-style-type: none"> <li>Accelerometer (Strain Gage and Servo Type)</li> <li>Velocity Transducer (Servo Type)</li> <li>Displacement Transducer (Inductance Type)</li> <li>Load Cell (Electrical Charge Type)</li> </ul>
Computer	PC-9801FS with Math Coprocessor (NEC)
Actuator	<ul style="list-style-type: none"> <li>Hydraulic Type Capacity : 300kgf</li> <li>Stroke : <math>\pm 100</math>mm Max. Velocity : 100kine</li> <li>Frequency : 0.5~10Hz</li> </ul>

## EXPERIMENTAL PROCEDURE

### Flow of Control Signals

Figure 5 shows the building model and testing device used in the shaking table test and the positions of the sensors. The actuator was installed between the uppermost floor of the building model and the reaction frame. This testing system was adopted in order to verify the control logic experimentally, because of its simplicity. Furthermore, it is confirmed that the simulated uncontrolled response is reproduced approximately under the uncontrolled condition with the actuator activated as shown in Figure 6. The actual systems to generate the active control force can be realized by extendedly using several conventional mechanisms such as active mass damper or tendon system.

### Specifications of the Building Model and Control Facilities

The building model is a two-story steel structure consisting of floors and columns (shown in Figure 5). The natural frequency is 1.312 Hz. The damping ratio is 0.211 % and the spring constant of a column is 0.3685 tf/cm, for each stories. Table 1 shows the specifications of the model, and Table 2 shows the specifications of the major components of the vibration control system, namely, sensors, personal computers, and actuator.

### Determination of Test Parameters

The MF was defined as shown in Fig. 3, where the ordinate  $\mu$  is the degree of satisfaction. If  $\mu=1$ , then both Y and U are at acceptable levels, but they become less acceptable as  $\mu$  approaches zero. In these experiments, the initial values of  $\alpha$  were set at 0.99 to reduce the inertia force due to the input of the initial earthquake motion.

### Input Earthquake Motion

To investigate the effect of seismic control on building response, two past earthquake ground motions were used in both the shaking table tests and the simulations: 1940 El Centro NS , 1952 Taft EW.

## RESULTS AND DISCUSSIONS

Tables 3 and 4 compares the measured and calculated  $Y_m$  values (the maximum response displacement of the uppermost floor), where A is the ratio of the measured  $Y_m$  for the controlled condition to that for the uncontrolled condition, B is that for the calculated  $Y_m$ , and C is the ratio of A/B. In Tables 3 and 4, the  $Y_m$  is calculated by the model of 2-degrees-of-freedom-system as shown in Eqs. (1)-(4).

### Influence of Membership Function (MF)

Tables 3 and 4 show  $Y_m$  for various MF. In Table 3, the MF for controlling force U is fixed, namely,  $U_1=0$ ,  $U_2=100$  (kgf) in Figure 4(b). The  $Y_m$  with a Type-1 MF was reduced to a greater degree than that with a Type-2 and Type-3 MF, even though the response conditions were severe with a Type-1 MF. The response reduction with a Type-2 MF was less than that with a Type-3 MF. The Type-2 MF has an interval of  $\mu=1$ , which allows a comparatively large response displacement.

In Table 4, the MF for Y is fixed, namely,  $Y_1=0$ ,  $Y_2=1.5$  (cm) as shown in Figure 4(a). The  $Y_m$  with a Type-3 MF, in which controlling forces were larger comparatively, was reduced to a greater degree than that with a Type-1 and Type-2 MF.

### Comparison between Experiment and Simulation

In Tables 3,4, the tendency that the values of A/B are smaller than or nearly equal to 1.00, shows that the reducing effect of the results by numerical simulation is equal to or less than that by experiment.

**Table 3 Experimental and Simulated Results:Part 1**

Effects of Membership Function of Response Displacement  
 Membership Function for Control Force is constant : U1=0, U2=100 kgf

Membership functions for response displacement Y(cm) of uppermost floor	Maximum acceleration of earthquake motions (cm/s <sup>2</sup> )	Maximum response displacement Ym(cm) of uppermost floor (controlled/uncontrolled)	
		El Centro NS	Taft EW
 Type-1	30	70818	70820
		0.397 (0.294)	0.373 (0.265)
		0.460 (0.359)	0.361 (0.270)
 Type-2	30	0.819	0.981
		70834	70836
		0.592 (0.439)	0.510 (0.362)
 Type-3	30	0.703 (0.526)	0.803 (0.600)
		0.835	0.603
		70826	70828
 Type-3	60	0.523 (0.387)	0.431 (0.306)
		0.555 (0.415)	0.478 (0.357)
		0.933	0.857
 Type-4	60	70912	70914
		0.957 (0.390)	0.972 (0.390)
		1.179 (0.503)	0.890 (0.384)
 Type-4	60	0.775	1.02
		70936	70938
		1.299 (0.529)	1.217 (0.488)
 Type-4	60	1.359 (0.580)	1.598 (0.889)
		0.912	0.708

Experiment Case Number
Max. resp. disp. by experiment (controlled/uncontrolled by experiment) = A
Max. resp. disp. by simulation (controlled/uncontrolled by simulation) = B
C = A / B

**NUMERICAL SIMULATION**

In this paper, two types of numerical simulations were conducted. One is the simulation for 2-degrees-of-freedom-system as shown in Equations (1)-(4) (2-deg-simulation), and the other is that for 5-degrees-of-freedom-system as shown in Figure 7 (5-deg-simulation) and Equation (16). In Figure 7, m<sub>R</sub> is the mass of reaction frame and piston of actuator, P<sub>1</sub> and P<sub>2</sub> is the oil pressure in the cylinder. The difference of the oil pressure P(=P<sub>1</sub>-P<sub>2</sub>), and Q<sub>b</sub> (the amount of running oil) are the variables besides y<sub>1</sub>, y<sub>2</sub>, and y<sub>R</sub> in the 5-deg-simulation.

In Figures 8 and 9, the response displacements of uppermost floor or second floor and their fourier spectra are compared respectively, among (a)experiment, (b)2-deg-simulation and (c)5-deg-simulation, in case of moderate control condition and severe control condition. In the case of moderate control condition (Figure 8), the results of uppermost floor by the 2-deg-simulation are similar to that of experiment, on the other hand, the response of second floor is more quantitatively and qualitatively evaluated by the 5-deg-simulation. In the case of severe control condition (Figure 9), the results of uppermost floor by 5-deg-simulation are similar to that of experiment, and it seems difficult to evaluate the response of second floor by both methods of simulation.

**CONCLUSIONS**

This paper outlined the shaking table tests for an active seismic response control system that uses fuzzy optimal logic (FOL). The test results confirmed the validity of the vibration control effect of this FOL control system, and demonstrated that its effectiveness can be increased by modifying the membership

**Table 4 Experimental and Simulated Results: Part 2**

Effects of Membership Function for Controlling Force MF for Resp. Disp. is const. : Y1=0, Y2=1.5 cm

Membership functions for controlling force U(kgf)	Maximum response displacement Ym(cm) of uppermost floor (controlled/uncontrolled)	
	El Centro NS	Taft EW
 Type-1	70846	70848
	0.469 (0.347)	0.412 (0.293)
	0.571 (0.427)	0.469 (0.351)
 Type-2	0.813	0.835
	70818	70820
	0.397 (0.294)	0.373 (0.265)
 Type-3	0.480 (0.359)	0.361 (0.270)
	0.819	0.981
	70850	70852
 Type-3	0.294 (0.218)	0.262 (0.186)
	0.380 (0.284)	0.281 (0.210)
	0.768	0.886

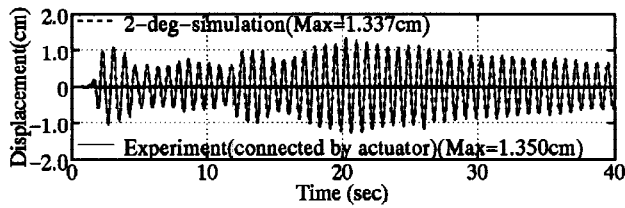


Fig.6 Uncontrolled Responses(EI Centro NS 30gal)

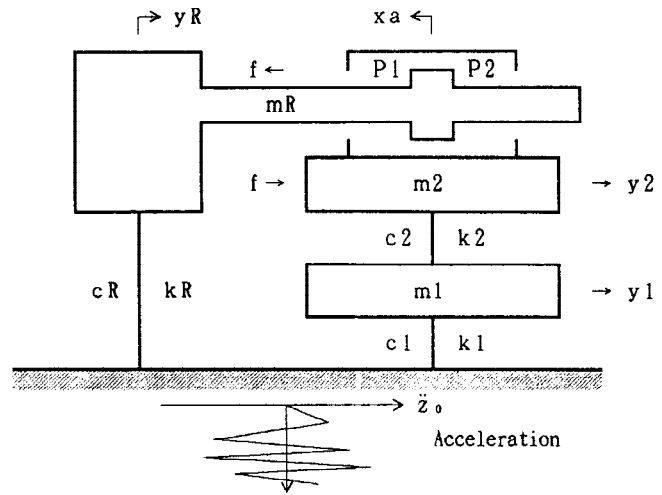


Fig.7 5-Degrees-of-Freedom System

$$\begin{aligned}
 & \begin{bmatrix} m_2 & 0 & 0 & 0 & 0 \\ 0 & m_1 & 0 & 0 & 0 \\ 0 & 0 & m_R & 0 & 0 \\ 0 & 0 & 0 & 0 & 0 \\ 0 & 0 & 0 & 0 & 0 \end{bmatrix} \begin{Bmatrix} \dot{y}_2 \\ \dot{y}_1 \\ \dot{y}_R \\ \dot{Q}_b \\ \dot{P} \end{Bmatrix} + \begin{bmatrix} c_2 & -c_2 & 0 & 0 & 0 \\ -c_2 & c_1 + c_2 & 0 & 0 & 0 \\ 0 & 0 & c_R & 0 & 0 \\ 0 & 0 & 0 & T & 0 \\ 2AK_\beta & 0 & -2AK_\beta & 0 & V_c \end{bmatrix} \begin{Bmatrix} \dot{y}_2 \\ \dot{y}_1 \\ \dot{y}_R \\ \dot{Q}_b \\ \dot{P} \end{Bmatrix} \\
 & + \begin{bmatrix} k_2 & -k_2 & 0 & 0 & -A \\ -k_2 & k_1 + k_2 & 0 & 0 & 0 \\ 0 & 0 & k_R & 0 & A \\ K_b K_v K_s & 0 & -K_b K_v K_s & 1 & K_b K_d \\ 0 & 0 & 0 & -2K_\beta & 2K_g K_\beta \end{bmatrix} \begin{Bmatrix} y_2 \\ y_1 \\ y_R \\ Q_b \\ P \end{Bmatrix} = \begin{Bmatrix} -m_2 \ddot{z}_0 \\ -m_1 \ddot{z}_0 \\ -m_R \ddot{z}_0 \\ K_b K_v v \\ 0 \end{Bmatrix} \quad \dots(16)
 \end{aligned}$$

function. Because seismic response control became ineffective under certain conditions, there is a need for improvement, such as incorporating the response of the second floor to handle higher mode vibration. These tests also demonstrated that the results of seismic response control tests can be qualitatively evaluated by a rather simple method of simulation. On the other hand, under the severe control condition, the test results of uppermost floor can be evaluated by the simulation for 5-degrees-of-freedom system.

### ACKNOWLEDGEMENTS

Authors express sincere thanks to Mr. Namihiko INOUE, a Researcher of Building Research Institute.

### REFERENCES

- [1]Tani,A. and H. Kawamura. Fuzzy Optimal Seismic Control System of Building - In Case of Active Equivalent Variable Mass System -, Proc. of the Second International Symposium on Uncertainty Modeling and Analysis, Apr. 1993, pp.611-618.
- [2]Kawamura,H., A. Tani, K. Tsunoda and M. Yamada. Real Time Prediction of Earthquake Ground Motions and Structural Response by Statistic and Fuzzy Logic, Proceedings of 8th Japan Earthquake Engineering Symposium, 1990, pp.1881-1886.
- [3]Kawamura,H. and J.T.P. Yao. Application of Fuzzy Logic to Structural Control Motion of Civil Engineering Structures,Proc.of NAFIPS,1990,pp.67-70.

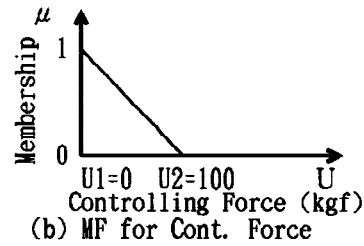
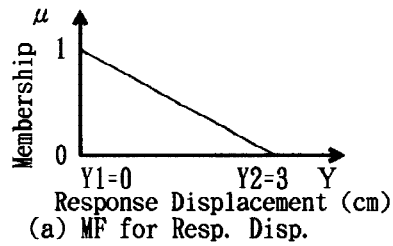


Fig.8.1 Membership Function (Moderate Control)

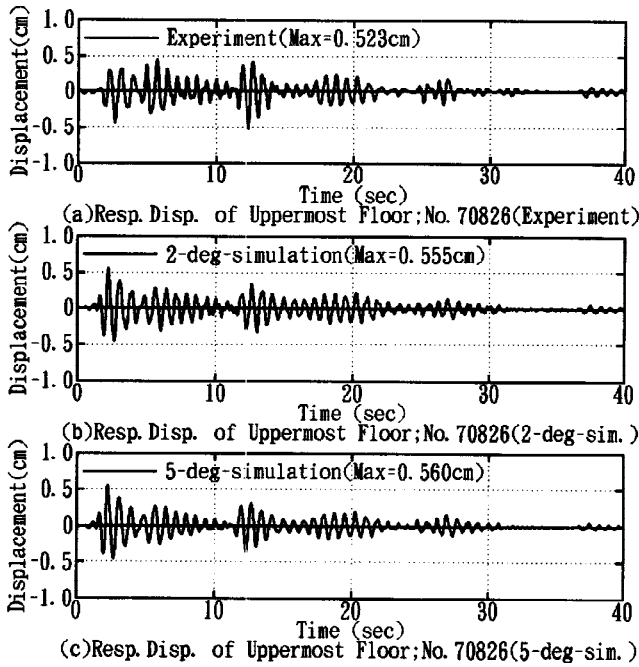


Fig.8.2 Response Displacement of Uppermost Floor by Moderate Control

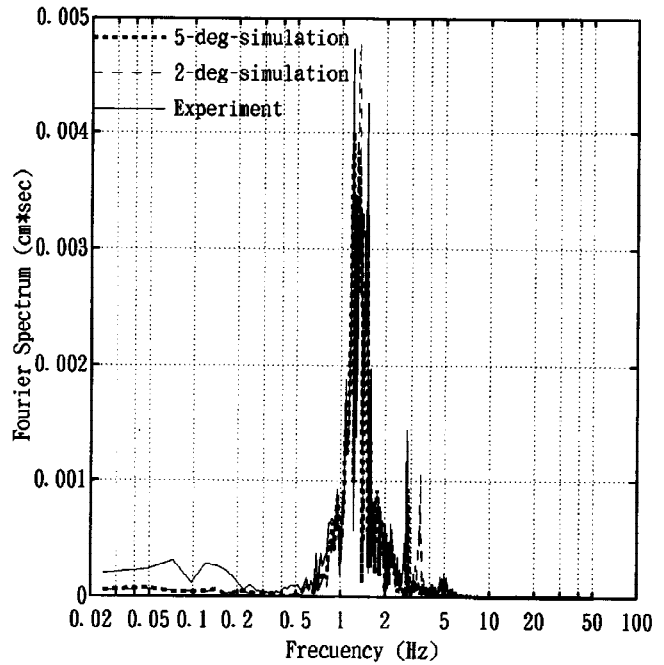


Fig.8.4 Fourier Spectra of Resp. Disp. of Uppermost Floor by Moderate Control

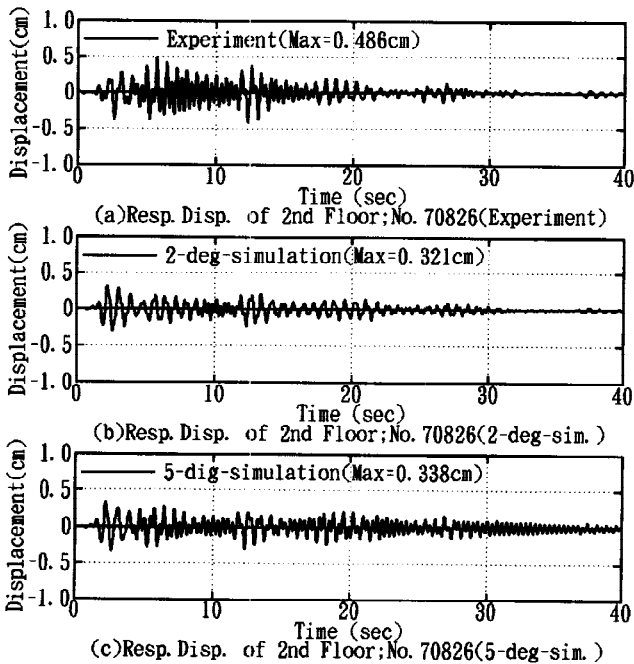


Fig.8.3 Response Displacement of Second Floor by Moderate Control

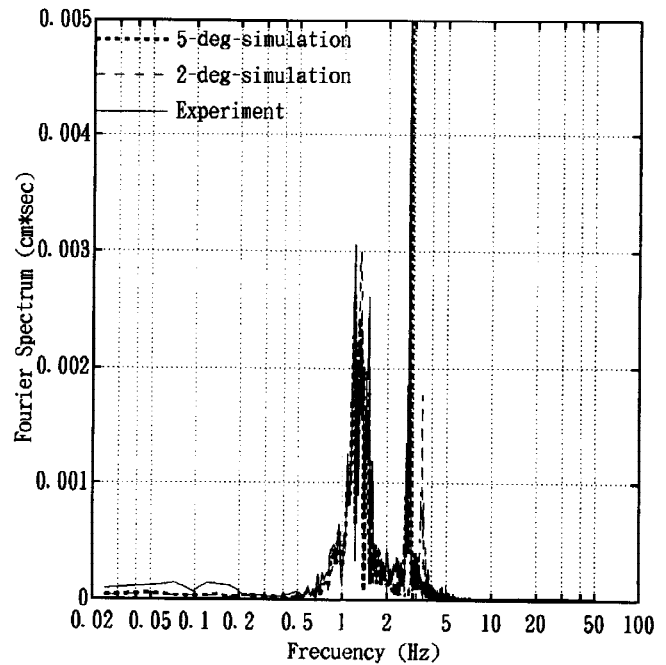


Fig.8.5 Fourier Spectra of Resp. Disp. of Second Floor by Moderate Control

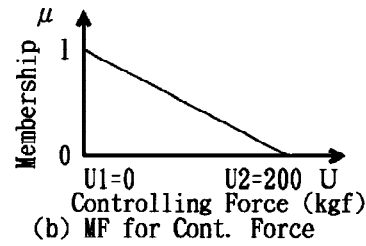
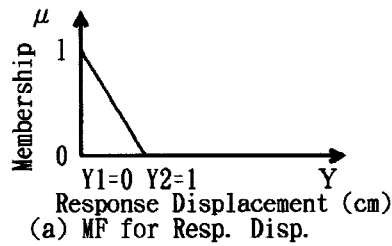


Fig.9.1 Membership Function (Severe Control)

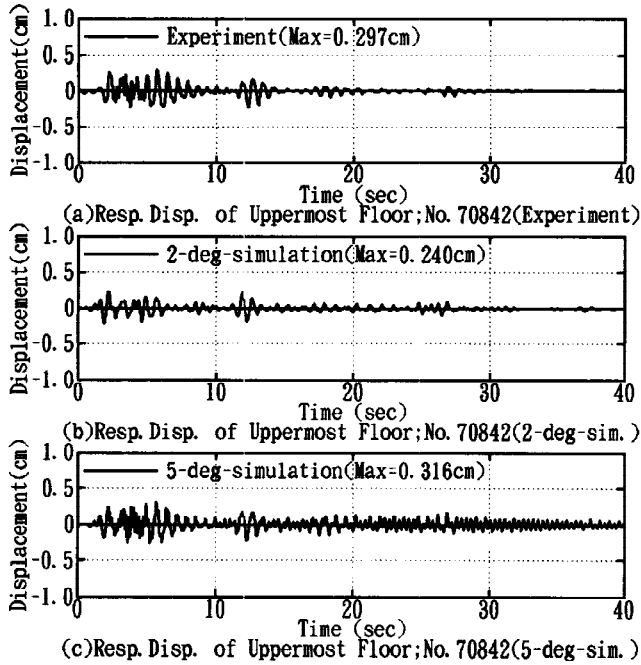


Fig.9.2 Response Displacement of Uppermost Floor by Severe Control

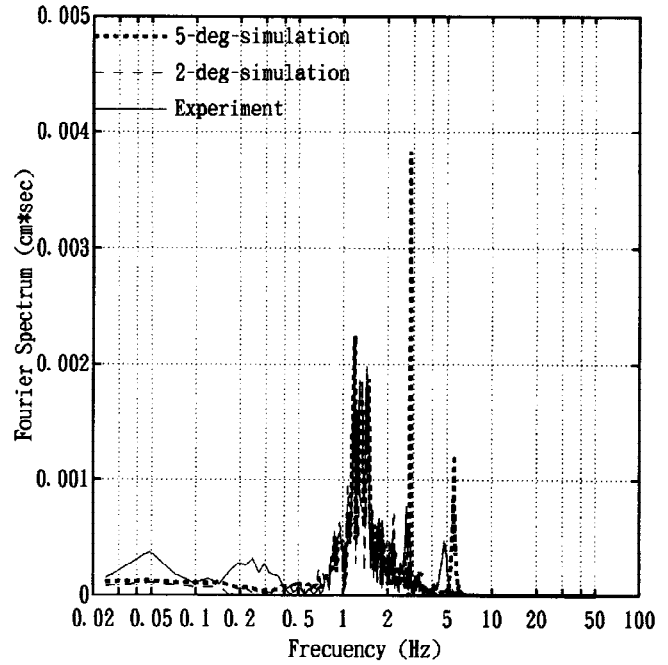


Fig.9.4 Fourier Spectra of Resp. Disp. of Uppermost Floor by Severe Control

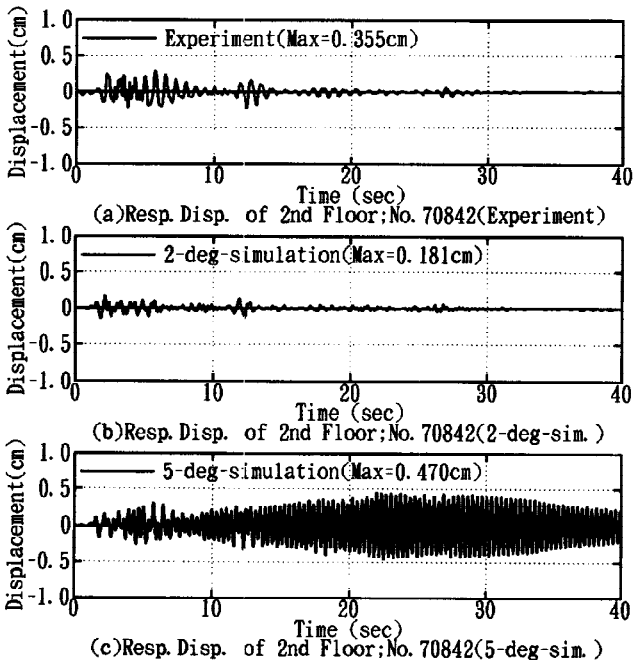


Fig.9.3 Response Displacement of Second Floor by Severe Control

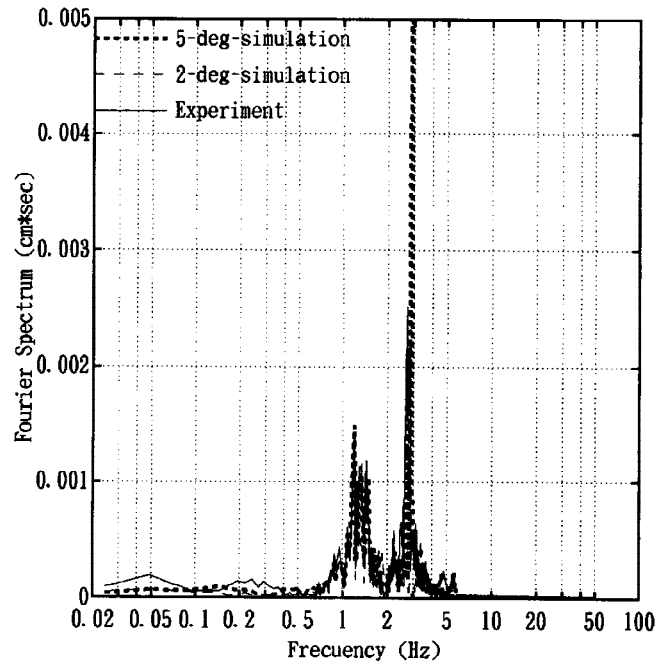


Fig.9.5 Fourier Spectra of Resp. Disp. of Second Floor by Severe Control